Supplementary Material for

Enhanced NH_3-SCR Activity of Cu-SAPO-34 by Regulating Si Distribution via an Interzeolite Conversion Strategy

Yuxuan Xiao[a], Bohui Cai[b], Huifang Wu[a], Hui Wang[c], Jiachen Wang[c], Junyan Liu[b], Runyu Ma[a], Tianming Lv[d], Lei Miao[a], Jiaxu Liu[c], Chengyang Yin[b, *], Changgong Meng [a, e, *], Limin Ren[a, *]

[a] *School of Chemistry, Dalian University of Technology, Dalian 116024, China*

[b] *Institute of Catalysis for Energy and Environment, College of Chemistry and Chemical Engineering, Shenyang Normal University, Shenyang 110034, China*

[c] *School of Chemical Engineering, Dalian University of Technology, Dalian 116024, China*

[d] *Instrumental Analysis Center, Dalian University of Technology, Dalian 116024, China*

[e] *College of Environmental and Chemical Engineering, Dalian University, Dalian 116622, China*

[*] *Corresponding authors*

E-mails: chengyang_yin@163.com (C. Yin), cgmeng@dlut.edu.cn (C. Meng), lren@dlut.edu.cn (L. Ren)

Experiment section

Chemicals

All chemicals were used as received without further treatment. Phosphoric acid (85 wt%) was purchased from Damao chemical reagent factory. Hydrated aluminum oxide (pseudo-bauxite, 70 wt% Al_2O_3) and silica sol (30 wt%) were purchased from Jinghuoglass company. Tetramethylammonium hydroxide ($TMAOH{\cdot}5H_2O$, 98 wt%), tetrapropylammonium hydroxide (TPAOH, 40 wt%) and hexamethyleneimine (HMI) were purchased from Energy chemical. Fumed silica was purchased from Cab-o-sil M5. $CuSO_4{\cdot}5H_2O$ was purchased from Tianjin Tianli chemical reagent company. Tetraethylenepentamine (TEPA) was purchased from Macklin reagent. Morpholine (MOR, 99 wt%) was purchased from Adamas-beta. Diethylamine (DEA) was purchased from Aladdin Industrial Corporation.

Synthesis of SAPO-37

To synthesize SAPO-37, solution A consisted of phosphoric acid (85 wt%), deionized water, and hydrated aluminum oxide (pseudo-bauxite, 70 wt% Al_2O_3), was stirred at room temperature for 8 h. Solution B with tetramethylammonium hydroxide ($TMAOH{\cdot}5H_2O$, 98 wt%), fumed silica, and tetrapropylammonium hydroxide (TPAOH, 40 wt%), was stirred for 1 h. Subsequently, solutions A and B were mixed and stirred for 24 h. To achieve samples with varying Si contents, the quantity of fumed silica was adjusted, resulting in a molar composition of the obtained mixture ranging from 0.3 ~ 1.3 SiO_2: Al_2O_3: P_2O_5: $(TPA)_2O$: 0.025 $(TMA)_2O$: 50 H_2O. The final gels were transferred to 50 mL stainless-steel autoclaves equipped with Teflon liners and heated at 200 °C for 13 h. The resulting product was then subjected to centrifugation using deionized water, followed by overnight drying at 60 °C. Subsequently, the dried samples were calcined at 600 °C for 10 h to remove the organic structure-directing agents. To obtain the waste catalyst SAPO-37, the calcined sample was stored at room temperature and in a humid environment for over 90 days, denoted as SAPO-37-W.

Synthesis of SAPO-37-S

To synthesize SAPO-37-S, a mixture consisting of hydrated aluminum oxide (pseudo-bauxite, 70 wt% Al_2O_3), phosphoric acid (85 wt%), tetrapropylammonium

hydroxide (TPAOH, 40 wt%), tetramethylammonium hydroxide ($TMAOH \cdot 5H_2O$, 98 wt%), and fumed silica was weighed and added to a mortar. The molar ratio was SiO_2: Al_2O_3: P_2O_5: $(TPA)_2O$: 0.025 $(TMA)_2O$: 38 H_2O, and the mixture was ground for 15 minutes until it reaches a uniform consistency. The resulting mixture was then transferred to 50 mL stainless-steel autoclaves fitted with Teflon liners and heated at 200 °C for 13 hours. The resulting product was subjected to centrifugation using deionized water and then undergoes overnight drying at 60 °C. Subsequently, the dried samples were calcined at 600 °C for 10 hours to eliminate the organic structure-directing agents. The resulting product was denoted as SAPO-37-S.

Synthesis of Cu-SAPO-34-IZC via interzeolite conversion

As a typical synthesis procedure of Cu-SAPO-34-IZC, $CuSO_4 \cdot 5H_2O$, tetraethylenepentamine (TEPA), and deionized water were first mixed and stirred for 15 min. Subsequently, hexamethyleneimine (HMI) was added and stirred at room temperature for 30 min until the mixture achieves complete uniformity. Finally, calcined SAPO-37 was added and stirred for 2 h. The resulting mixture was introduced into 50 mL stainless-steel autoclaves equipped with Teflon liners and heated at 180 °C for various durations. After hydrothermal crystallization, the sample was subjected to repeated centrifugation using deionized water. The sample was then dried overnight in an oven at 60 °C and subsequently calcined in a muffle furnace at 600 °C for 10 h to obtain Cu-SAPO-34.

Synthesis of Cu-SAPO-34-OP

First, 6.380 g of phosphoric acid (85 wt%) and 24.686 g of deionized water were mixed and stirred for 5 minutes. Then, 4.857 g of hydrated aluminum oxide (pseudo-bauxite, 70 wt% Al_2O_3) was added and stirred for 20 minutes. Next, 1.8 g of fumed silica was added and stirred for 30 minutes, followed by the addition of 5.808 g of morpholine (MOR, 99 wt%), which was added drop by drop and stirred for an additional 30 minutes. Finally, a solution composed of 0.607 g of $CuSO_4 \cdot 5H_2O$, 0.719 g of tetraethylenepentamine (TEPA), and 10.899 g of deionized water was added and aged at 500 rpm for 24 hours under stirring. The molar ratio was 0.114 Cu-TEPA: 2 MOR: 0.9 SiO_2: 0.83 P_2O_5: Al_2O_3: 60 H_2O. The resulting mixture was then transferred

to 50 mL stainless-steel autoclaves fitted with Teflon liners and heated at 200 °C for 3 days. The resulting product was subjected to centrifugation using deionized water and then undergoes overnight drying at 60 °C. Subsequently, the dried samples were calcined at 600 °C for 10 hours to eliminate the organic structure-directing agents. The resulting product was denoted as Cu-SAPO-34-OP.

Synthesis of Cu-SAPO-34-IE

First, SAPO-34 was synthesized. Solution A was prepared by mixing and stirring hydrated aluminum oxide (pseudo-bauxite, 70 wt% Al_2O_3), deionized water, and phosphoric acid (85 wt%) for 2 hours. Silica sol (30 wt%) and diethylamine (DEA) were mixed and stirred for 2 hours to obtain solution B. Subsequently, solution B was added drop by drop to solution A and stirred for 2 hours, with a molar ratio of 2 DEA: 0.6 SiO_2: Al_2O_3: 0.8 P_2O_5: 50 H_2O. The resulting gel was transferred to a Teflon lined stainless steel autoclave and heated at 200 °C for 3 days. The resulting solid product was centrifuged in deionized water and calcined in a muffle furnace at 600 °C for 10 hours to remove the organic structure-directing agents. The calcined SAPO-34 was stirred in a 0.01 mol/L $CuSO_4$ solution at 50 °C for 1 hour. After centrifugation to collect the sample, it was calcined in a muffle furnace at 500 °C for 4 hours. These procedures were repeated twice to ensure thorough ion exchange. The final product obtained was named Cu-SAPO-34-IE.

Hydrothermal aging

To evaluate the hydrothermal stability of the Cu–SAPO-34 samples, the catalysts were subjected to hydrothermal treatment at 750 °C for 12 hours under a 10% H_2O/air flow.

Characterization

Powder X-ray diffraction (XRD) analyses were performed on a Bruker D8 Advance X-ray diffractometer in the scanning range of 2θ between 5° and 40° using copper Kα as the source of radiation (λ=1.5418 Å). N_2 adsorption-desorption isotherms were measured using a Micromeritics 3Flex instrument at -196 °C. All samples were vacuum degassed at 200 °C for 5

h before measurement. Total surface area was evaluated using the BET equation. UV-vis spectra were recorded in the range of 192–800 nm on a JASCO UV-550 spectrometer. ICP-OES was performed using a PerkinElmer AVIO 500. 10 mg of sample was dissolved in hydrofluoric acid and diluted to 25 mL with water. The CHN analysis was carried out on Elementar UNICUBE/OXYCUBE elemental analyzer. Scanning electron microscope (SEM) images were obtained with the electron microscope JEOL JSM-7900F Plus. Fourier Transform infrared spectroscopy (FTIR) was measured on a ThermoFisher 6700 with KBr pellets. ^{29}Si MAS NMR spectra were recorded on Agilent DD2-500 MHz (B0=11.7 T) spectrometer. ^{29}Si MAS NMR used a 6 mm probe with a resonance frequency of 99.29 MHz and a rotation speed of 4 KHz, and used high power proton decoupling. Samples were collected 1000 times under 4 s relaxation time and kaolin was used as the standard sample. Transmission Electron Microscope (TEM) images were obtained with the electron microscope JEOL JEM-F200. H_2-TPR experiments were performed on a PCA-1200 chemisorption analyzer. The samples were pre-treated in Ar flow (30 mL/min) at 300 °C for 0.5 h, then the TPR experiments were conducted in a 10% H_2/Ar atmosphere with a flow rate of 30 mL/min. The temperature was ramped linearly from 60 °C to 900 °C at a rate of 10 °C/min, while hydrogen consumption was monitored using a TCD detector. Electron Paramagnetic Resonance (EPR) experiments were carried out on a Bruker A200 spectrometer. The samples were sealed in quartz tubes and pretreated at 120 °C in pure N_2 flow for 12 h. The spectra were collected at -173 °C. During the spectral collection, the microwave power was 4.93 mW and the frequency was 9.33 GHz. The sweep width was 1300 G and the sweep time was 168 s, modulated at 100 kHz with 2 G amplitude. A time constant of 41 ms was used. The infrared spectra of NO adsorption were obtained using home-made equipment equipped with MCT detectors, covering the range of 4000–400 cm^{-1} with an optical resolution of 4 cm^{-1}. The catalysts were mixed with KBr at a 1:20 mass ratio, pressed into thin wafers (approximately 50 mg per 1.5 cm^2), and placed in the sample beam of a dual-beam IR cell. The wafers were pretreated at 773 K for 2 h under high vacuum (5×10^{-3} Pa). Reference spectra were collected after the cell cooled to room temperature. Analytically pure formic acid vapor was introduced into the IR cell for 5 minutes. The catalysts were purged with flowing N_2 gas for 30 minutes and then desorbed by temperature ramping from 303 to 473 K. The series of adsorption spectra (sample beam) and gas reference spectra (reference beam) were

collected simultaneously as time-resolved spectra during the entire desorption process. The NH_3-TPD experiments were performed on a PCA-1200 chemisorption analyzer. The samples were pre-treated in Ar flow (30 mL/min) at 500 °C for 1 h and treated in a flow of 10% NH_3 and 90% Ar (30 mL/min) for 40 min at 150 °C to adsorb ammonia. Then samples were treated in Ar flow (30 mL/min) at 150 °C for 40 min to remove the physical adsorbed NH_3 molecules. Measurement of NH_3 desorption was performed from 120 to 650 °C (10 °C/min) under Ar flow (30 mL/min).

Catalysis evaluation

Thermofisher Nicolet iS50 FTIR spectroscopy was used to evaluate the denitration activity of NH_3-SCR reaction. NH_3-SCR test results were obtained by the reaction of the catalyst in the micro reactor, and the temperature was obtained by the thermocouple inserted into the catalyst. Firstly, place 0.1 g of catalyst in the middle of the quartz tube and fix it with quartz wool. After that, put the reaction tube with catalyst and thermocouple into the reaction furnace (the reaction tube should avoid air leakage and air intake), and close the reaction furnace. Then, the sample was pretreated at 500 ℃ for 2 h, and the heating rate was maintained at 5 ℃/min. Then the reaction tube was naturally cooled to room temperature and the background was collected. Finally, in the range of 100-550 ℃, the activity data of the catalyst were collected at a heating rate of 3 ℃/min. The total flow of gas was 100 mL/min, and the specific gas components and concentrations were as follows: taking N_2 as equilibrium gas, 5% O_2, 500 ppm NO, 500 ppm NH_3, 5 vol% H_2O (when used). The gas hourly space velocity (GHSV) was 40,000 h^{-1}. The conversion of NO is obtained by the following formula.

$$\text{NO Conversion (\%)} = \frac{[NO]_{in} - [NO]_{out}}{[NO]_{in}} \times 100\%$$

$$\text{N}_2\text{ Selectivity (\%)} = \left(1 - \frac{2[N_2O]_{out}}{[NO_x]_{in} + [NH_3]_{in} - [NO_x]_{out} - [NH_3]_{out}}\right) \times 100\%$$

Table S1 Optimizing synthetic conditions of Cu-SAPO-34

Sample[a]	Cu:TEPA[b]	TEPA/T[c]	HMI/T[c]	pH	Synthesis time (h)	Product Phase[d]
IZC-1	1:0	/	/	4.30	72	amor.
IZC-2	1:1	0.015	/	6.46	72	amor.
IZC-3	1:6.7	0.1	/	11.48	72	CHA
IZC-4	1:6.7	0.1	0.3	12.89	24	CHA
IZC-5	1:0	/	0.3	11.91	72	amor. + CHA
IZC-6	0:6.7	0.1	0.3	12.95	72	amor. + CHA
IZC-7[e]	1:6.7	0.1	0.3	12.89	12	CHA

[a] All samples were crystallized at 180 °C. [b] 1 means the Cu content in the gel of samples is 4.75 wt% of the starting zeolite; TEPA: tetraethylenepentamine. [c] T= P+ Al+ Si in SAPO-37; HMI: hexamethyleneimine. [d] Amor. is short for amorphous phase. [e] The starting zeolite is SAPO-37-S.

As shown in Table S1, In the absence of TEPA (sample IZC-1) or with a low TEPA feeding ratio (TEPA/T = 0.015, sample IZC-2), only amorphous products are obtained. In contrast, when Cu-TEPA is present within an appropriate range, pure-phase Cu-SAPO-34 can be synthesized with high crystallinity (samples IZC-3 and IZC-4, as shown in Fig. S1 and Table S2). Comparing samples IZC-4 and IZC-3, we conclude that the addition of HMI accelerates the growth of the zeolite by providing a higher pH in the synthesis gel. However, when only HMI is combined with Cu ions, the resulting product contains a significant amount of amorphous material (sample IZC-5, Fig. S1 and Table S2). Similarly, if HMI and TEPA are fed together without Cu source, the majority of the product remains amorphous (sample IZC-6, Fig. S1 and Table S2). Collectively, these results confirm the dominant structure-directing role of the Cu-TEPA complex, which matches well with the CHA cage.

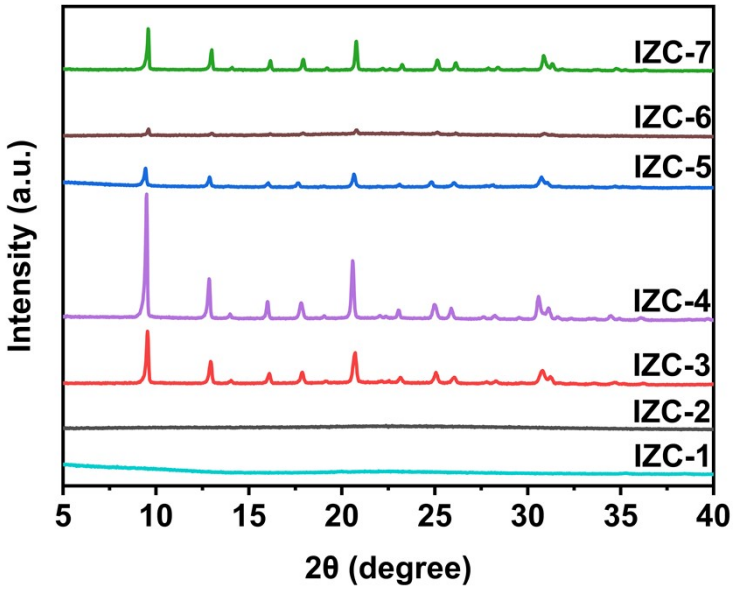

Fig. S1 XRD patterns of IZC-1, IZC-2, IZC-3, IZC-4, IZC-5, IZC-6 and IZC-7.

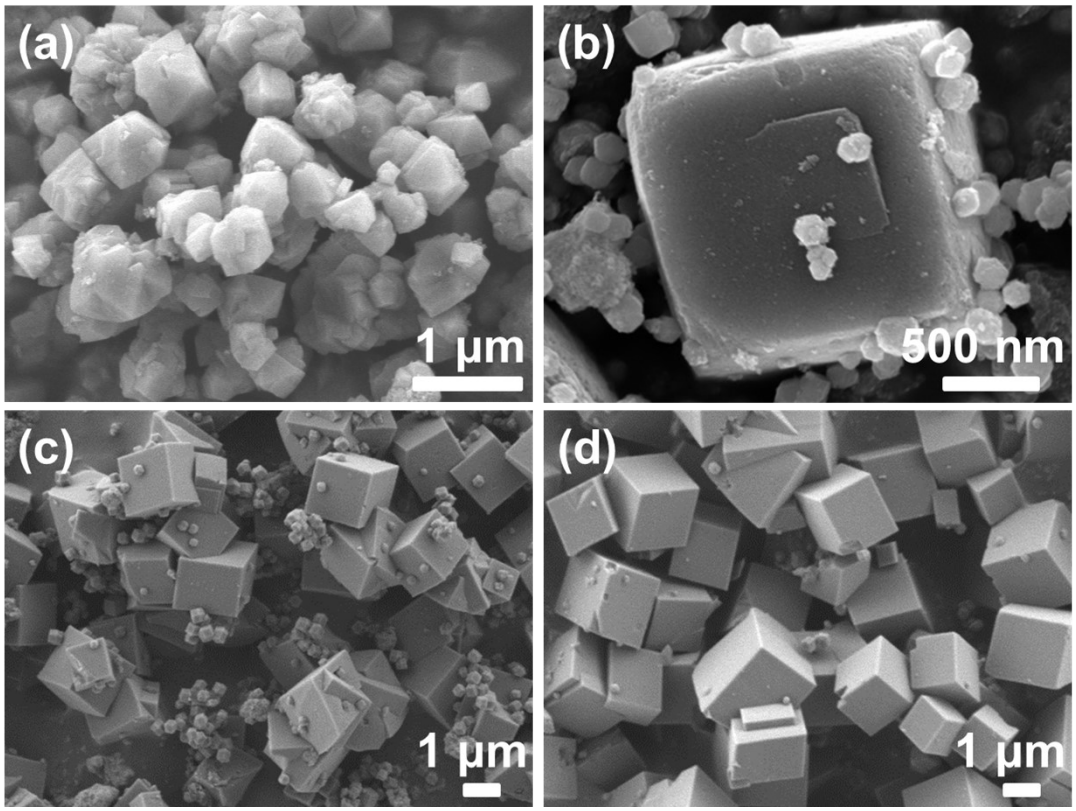

Fig. S2 SEM images of (a) SAPO-37-S and Cu-SAPO-34-IZC products obtained by interzeolite conversion at (b) 1 h, (c) 8 h and (d) 12 h.

SAPO-37-S, featuring a smaller crystal size of approximately 500 nm (Fig. S2a), was employed as the initial zeolite, it is concluded that high crystalline Cu-SAPO-34 can be obtained at 12 h (IZC-7, Fig. S1, Table S2). This experiment suggests that a parent zeolite with a smaller size is likely more conducive to the efficient degradation and release of these basic structural units, ultimately leading to a shorter crystallization time.

Table S2 Structural properties of the samples

Sample	Surface Area (m^2/g) [a]			Pore Volume (cm^3/g) [a]	
	S_{BET}	S_{micro}	S_{exter}	V_{total}	V_{micro}
IZC-1	/	/	/	/	/
IZC-2	/	/	/	/	/
IZC-3	164	145	19	0.09	0.06
IZC-4	659	647	12	0.27	0.26
IZC-5	152	132	20	0.10	0.05
IZC-6	40	3	37	0.09	0.01
IZC-7	734	660	74	0.36	0.25

[a] Surface area and pore volume were determined by *t*-plot method.

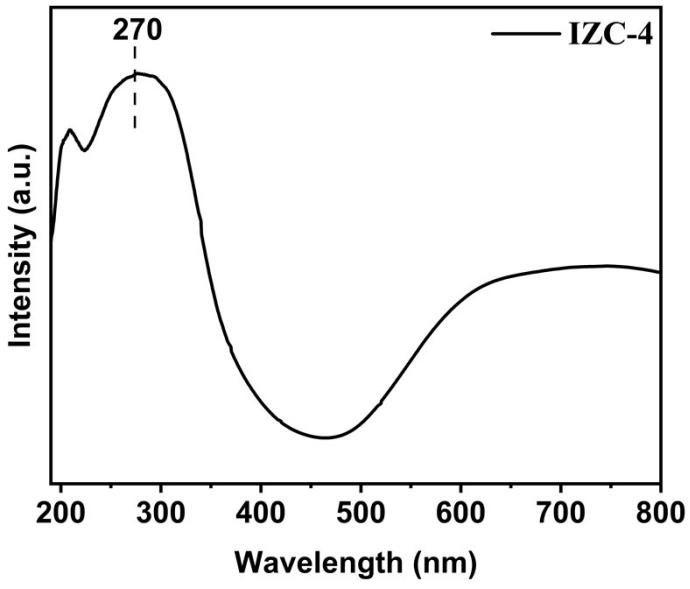

Fig. S3 UV-vis spectrum of as-synthesized IZC-4.

Table S3 Elemental analysis of as-synthesized IZC-4

Sample	$C/N_{theo.}$	C/N_{real}	TEPA (wt%)	HMI (wt%)
Cu-SAPO-34-IZC	2.64	2.71	9.36	8.33

C, H and N elemental analysis results (Table S3) of IZC-4 shows TEPA and HMI counted for 9.36 wt% and 8.33 wt% of the sample mass, respectively, the C/N ratio (2.71) of the as-synthesized sample is close to the theoretical C/N ratio (2.64), indicating both organic structure-directing agents (OSDA) filled in the micropores of the zeolite and acted together in the synthesis process.

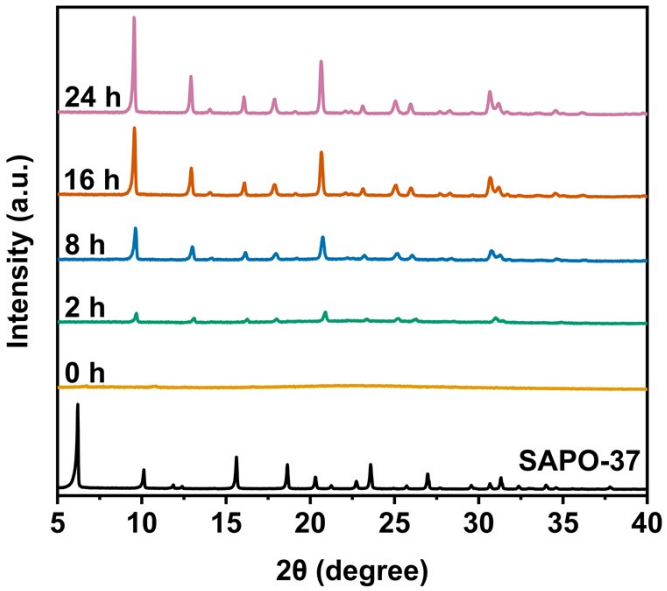

Fig. S4 XRD patterns of SAPO-37 and products obtained by interzeolite conversion (IZC) at different growth times.

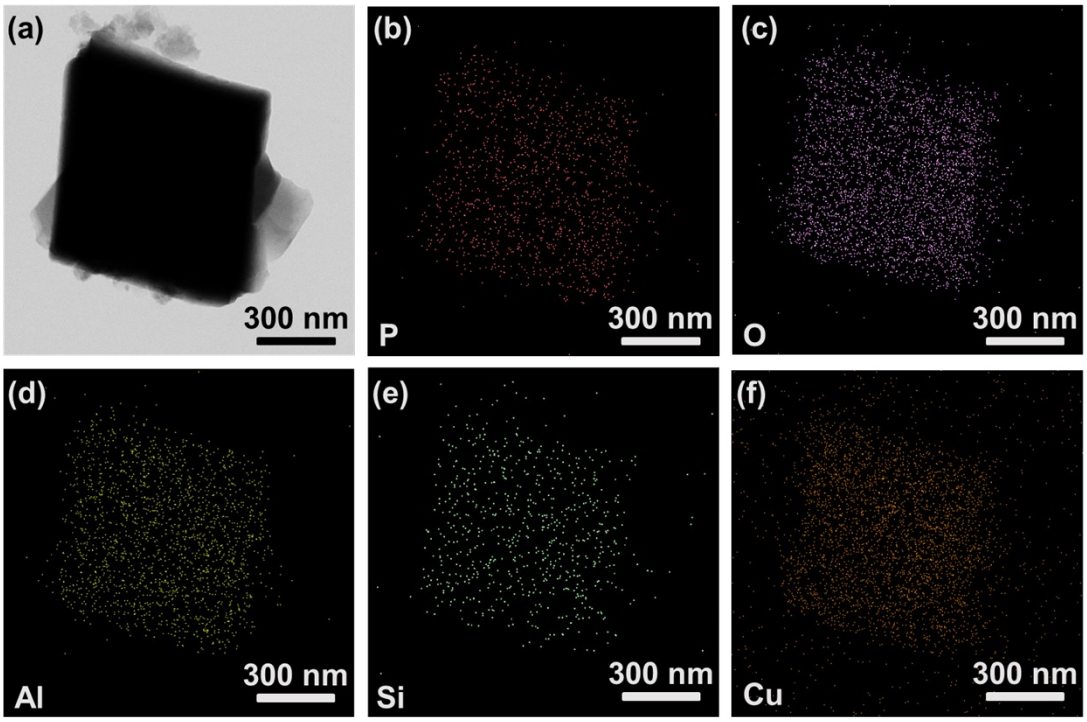

Fig. S5. TEM (a) and (b-f) EDS elemental mapping images of Cu-SAPO-34-IZC.

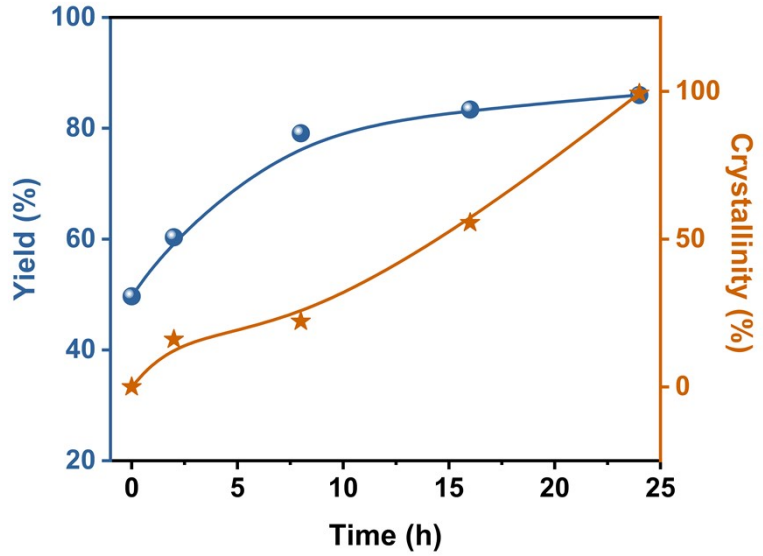

Fig. S6 Yield and relative crystallinity of Cu-SAPO-34-IZC obtained by interzeolite conversion at different growth times. (The relative crystallinity was determined by the sum of intensities of XRD peaks.)

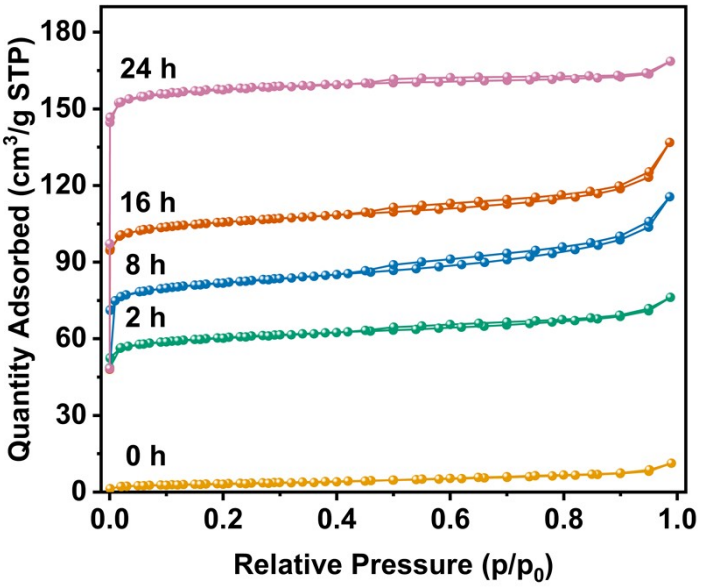

Fig. S7 N_2 adsorption-desorption isotherms of products obtained by IZC at different growth times.

Table S4 Structural properties and elemental analysis of the products obtained by interzeolite conversion at different growth times.

Sample	Surface Area (m^2/g) [a]			Pore Volume (cm^3/g) [a]		P/Al/Si/Cu [b]	Cu (wt%) [b]
	S_{BET}	S_{micro}	S_{exter}	V_{total}	V_{micro}		
0 h	12	1	11	0.02	/	1/0.93/0.30/0.01	0.1
2 h	231	200	31	0.12	0.08	1/1.10/0.38/0.04	1.5
4 h	300	262	38	0.16	0.11	1/1.15/0.38/0.05	1.7
8 h	311	268	43	0.18	0.11	1/1.30/0.46/0.05	1.8
16 h	407	368	38	0.21	0.15	1/1.15/0.37/0.04	1.5
24 h	659	647	12	0.27	0.26	1/1.08/0.35/0.04	1.4

[a] Surface area and pore volume were determined by *t*-plot method. [b] Determined by ICP analysis.

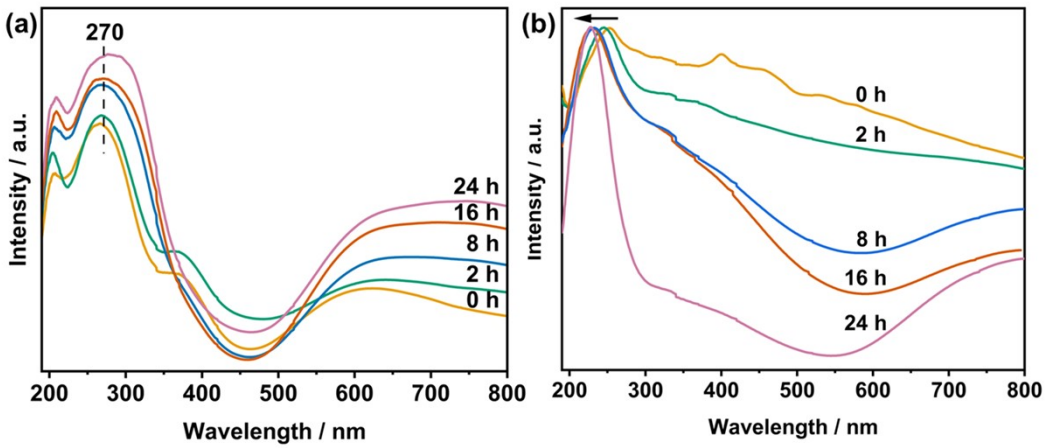

Fig. S8 UV-vis spectra of (a) as-synthesized Cu-SAPO-34-IZC products and (b) calcined Cu-SAPO-34-IZC products obtained by IZC at different growth times.

For the as-synthesized samples, the majority of Cu exists in the form of Cu-TEPA throughout the entire growth period (Fig. S8a). In contrast, for the calcined samples at various stages, as the CHA framework becomes more complete, we observe an increasing presence of isolated Cu^{2+}, indicated by the peak at 220 nm (Fig. S8b). This observation can be explained as follows: during the calcination of the early stage (0-16 h) samples, which have insufficient binding sites (Si-O-Al units), Cu-TEPA is forced to decompose into CuO, resulting in the formation of CuO_x species that are observed over a wide range of wavelengths (300-500 nm). As the framework matures and more binding sites provided by Si-O-Al units become available, a uniform isolated Cu^{2+} status is achieved, as reflected by the narrow and sharp peak at 220 nm (24 h). In summary, our analysis confirms that as the Cu-SAPO-34 framework matures, Cu-TEPA becomes encapsulated, ultimately resulting in isolated Cu^{2+} species that bind to Si-O-Al sites after calcination.

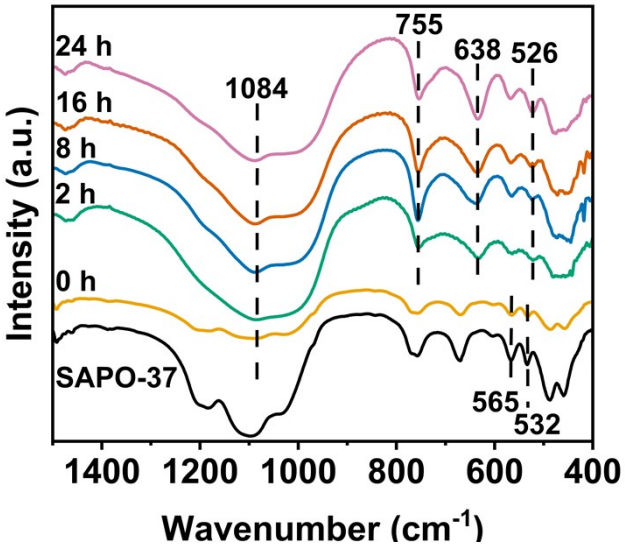

Fig. S9 FTIR spectra of SAPO-37 and Cu-SAPO-34-IZC products obtained by interzeolite conversion at different growth times.

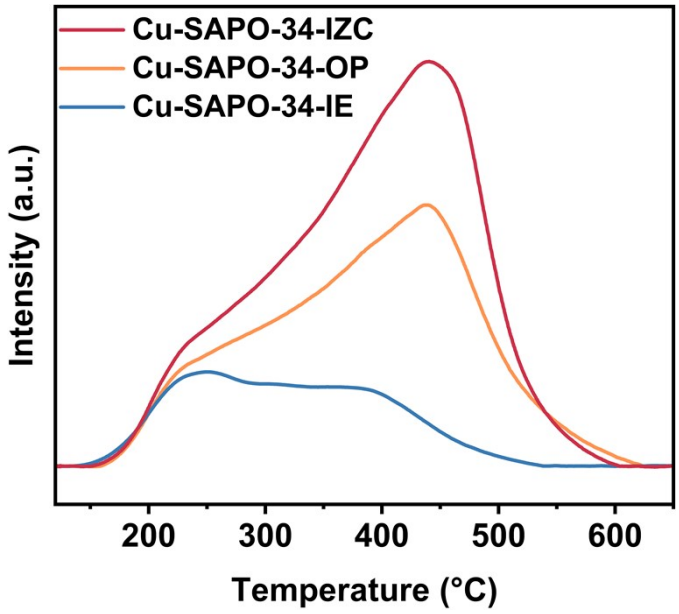

Fig. S10 NH_3-TPD profiles of Cu-SAPO-34-IZC, Cu-SAPO-34-OP and Cu-SAPO-34-IE.

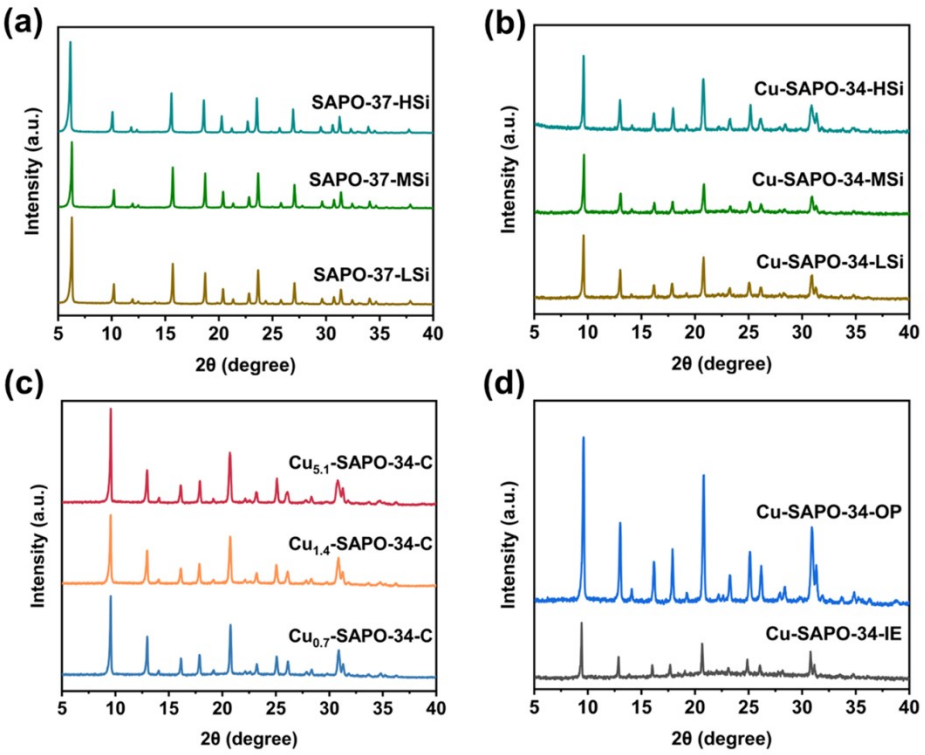

Fig. S11 XRD patterns of (a) SAPO-37 with different Si contents, (b) Cu-SAPO-34-IZC with different Si contents, (c) Cu-SAPO-34-IZC with different Cu contents and (d) Cu-SAPO-34-OP and Cu-SAPO-34-IE.

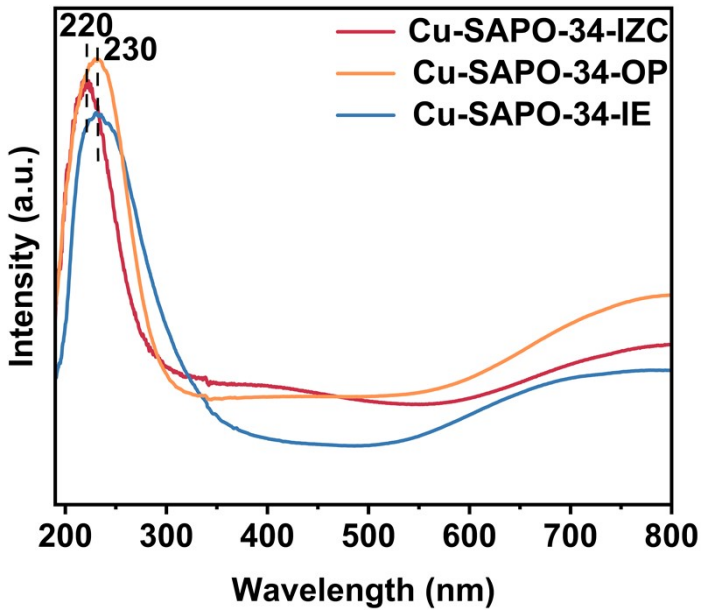

Fig. S12 UV-vis spectra of Cu-SAPO-34-IZC, Cu-SAPO-34-OP and Cu-SAPO-34-IE.

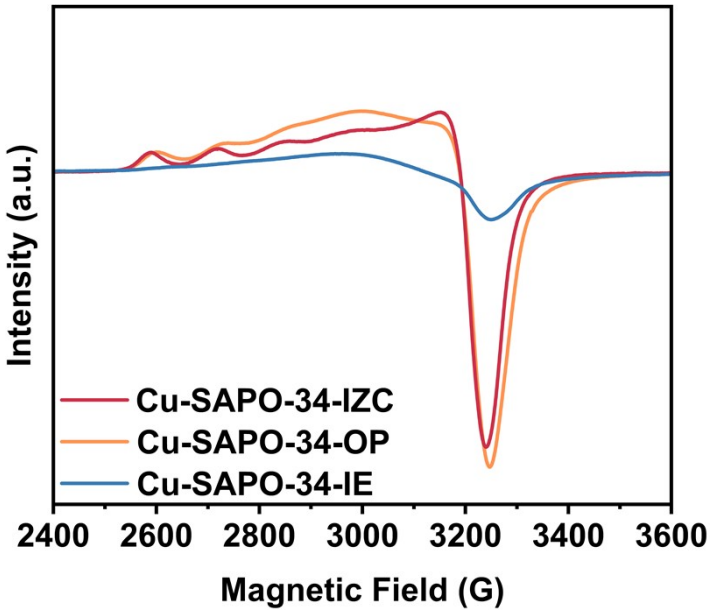

Fig. S13 EPR spectra of Cu-SAPO-34-IZC, Cu-SAPO-34-OP and Cu-SAPO-34-IE.

Table S5 Elemental analysis of Cu-SAPO-34 synthesized using different methods.

Sample[a]	Si (wt%)	Cu (wt%)
Cu-SAPO-34-IZC	5.7	1.4
Cu-SAPO-34-OP	5.8	1.7
Cu-SAPO-34-IE	3.3	0.7

[a] Determined by ICP analysis.

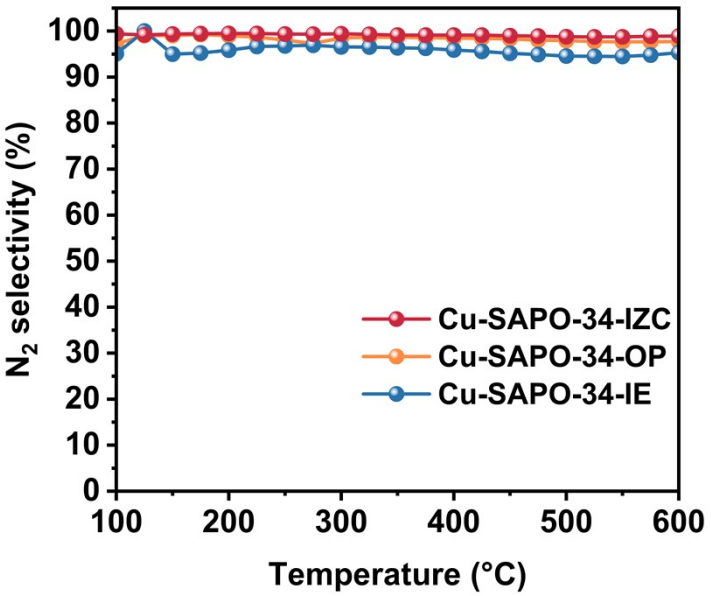

Fig. S14 N_2 selectivity as a function of temperature for Cu-SAPO-34-IZC, Cu-SAPO-34-OP and Cu-SAPO-34-IE. Reaction condition: 5% O_2, 500 ppm NO, 500 ppm NH_3, balance N_2, GHSV=40000 h^{-1}.

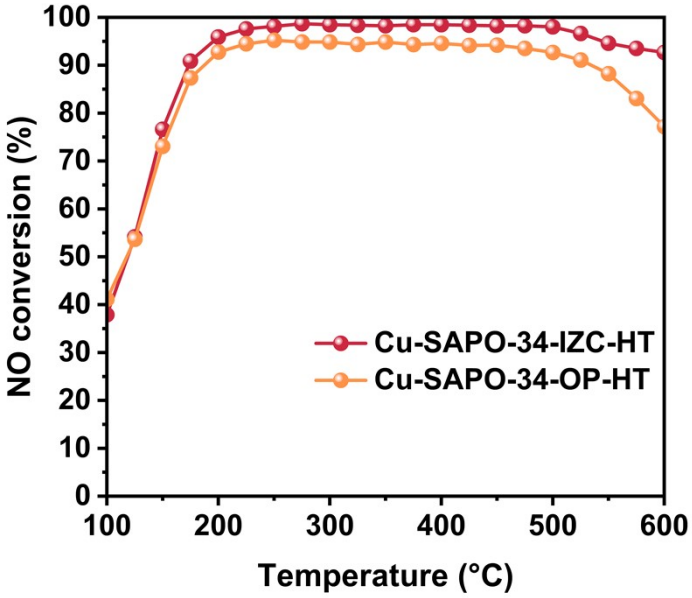

Fig. S15 NO conversion as a function of temperature for Cu-SAPO-34-IZC and Cu-SAPO-34-OP after 750 °C hydrothermal aging for 12 h. Reaction condition: 5% O_2, 500 ppm NO, 500 ppm NH_3, balance N_2, GHSV=40000 h^{-1}.

Table S6 Elemental analysis of samples.

Sample [a]	P/Al/Si/Cu	Si (wt%)	Cu (wt%)
SAPO-37-LSi	1/0.92/0.15	3.9	/
SAPO-37-MSi	1/0.94/0.18	4.3	/
SAPO-37-HSi	1/1.03/0.22	4.6	/
Cu-SAPO-34-LSi	1/1.03/0.17/0.03	4.9	1.5
Cu-SAPO-34-HSi	1/1.06/0.34/0.03	6.2	1.4
$Cu_{5.1}$-SAPO-34-IZC	1/1.51/0.42/0.18	5.7	5.1
$Cu_{0.7}$-SAPO-34-IZC	1/1.62/0.39/0.02	5.8	0.7

[a] Determined by ICP analysis.

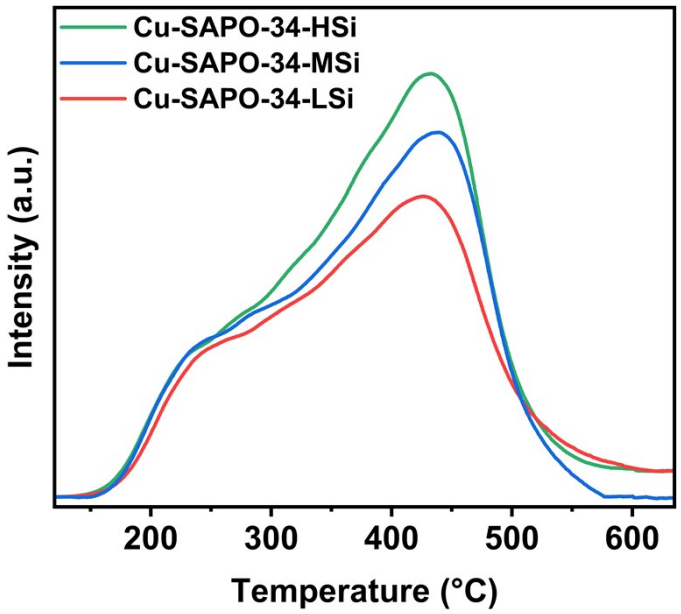

Fig. S16 NH_3-TPD profiles of Cu-SAPO-34-IZC with different Si contents.

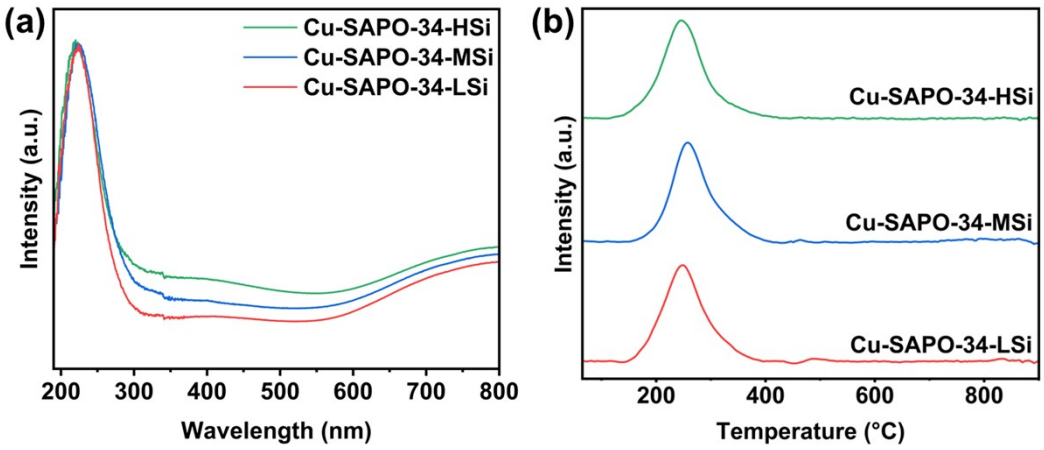

Fig. S17 (a) UV-vis spectra and (b) H_2-TPR curves of Cu-SAPO-34-IZC with different Si contents.

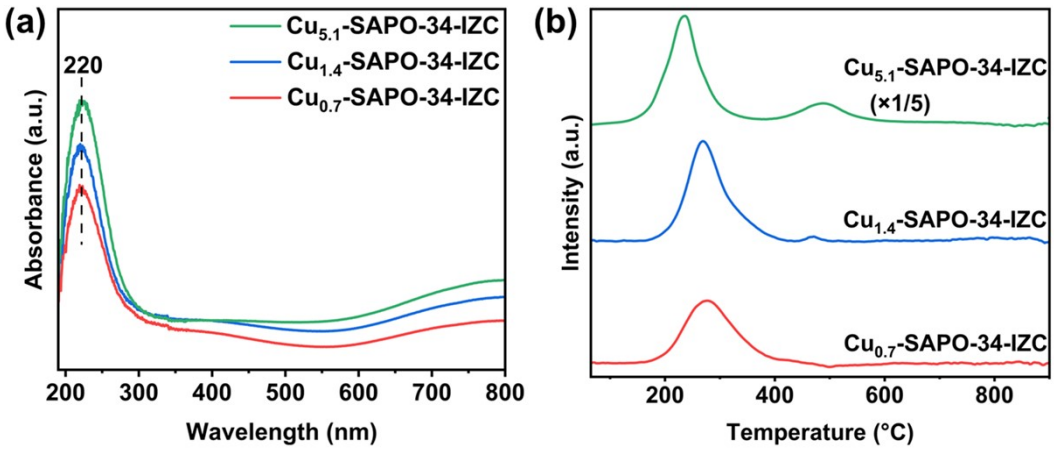

Fig. S18 (a) UV-vis spectra and (b) H_2-TPR curves of Cu-SAPO-34-IZC with different Cu contents.

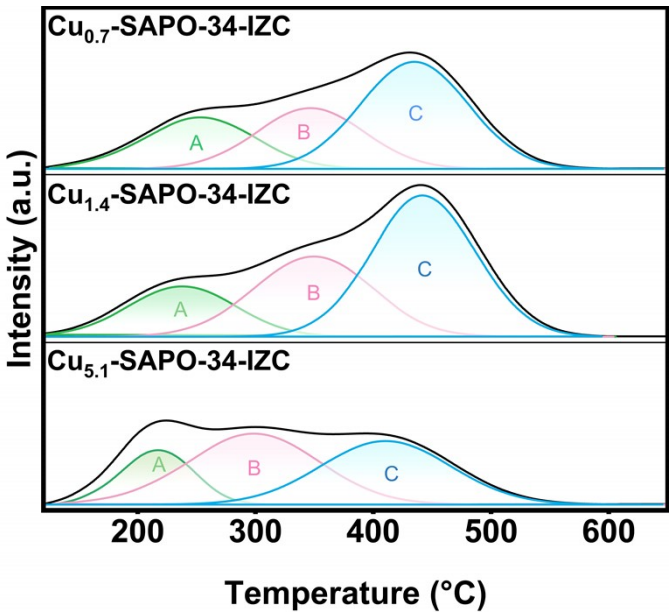

Fig. S19 NH_3-TPD profiles of Cu-SAPO-34 with different Cu contents.

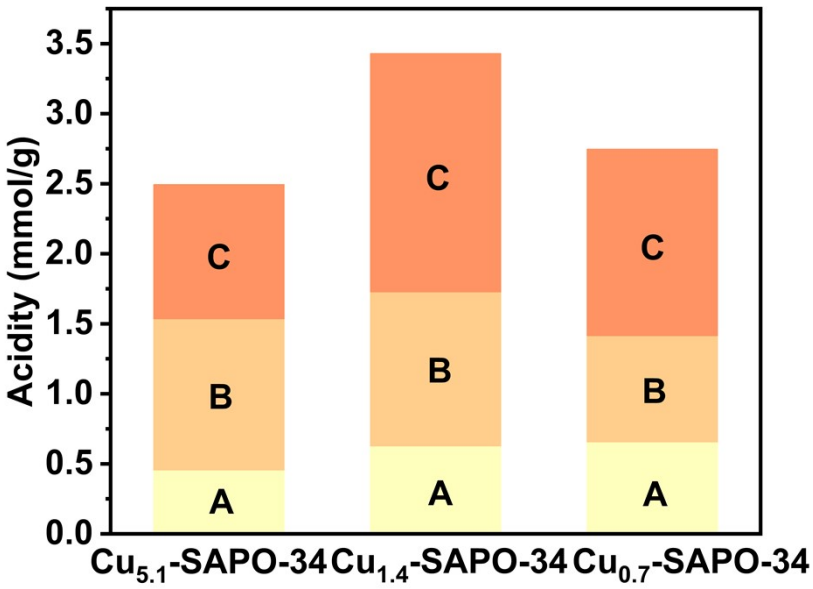

Fig. S20 Integrated NH_3 desorption amounts from NH_3-TPD results of Cu-SAPO-34-IZC with different Cu contents. (The areas of regions A, B, and C represent the amounts of ammonia desorption corresponding to peaks centered at 220 °C, 350 °C, and 440 °C, respectively.)

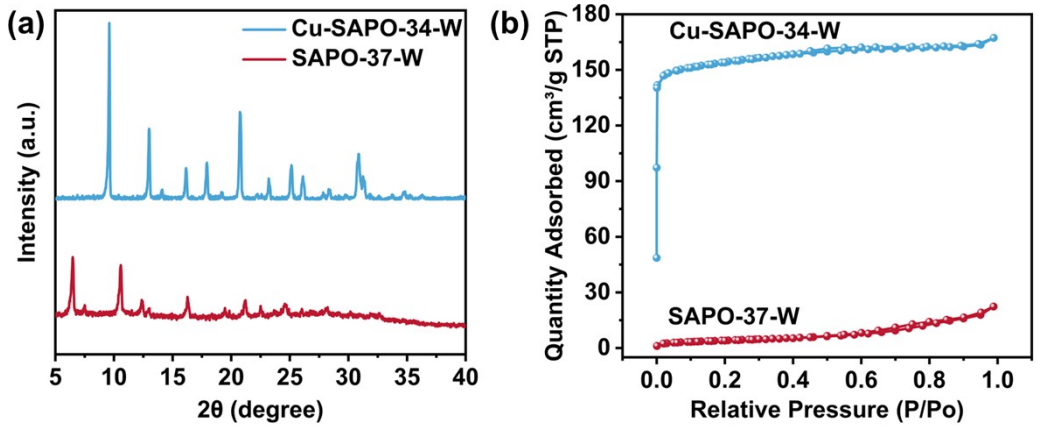

Fig. S21 (a) XRD patterns and (b) N_2 adsorption-desorption isotherms of SAPO-37-W and Cu-SAPO-34-W.

Table S7 Structural properties of SAPO-37-W and Cu-SAPO-34-W.

Sample	Surface Area (m^2/g) [a]			Pore Volume (cm^3/g) [a]	
	S_{BET}	S_{micro}	S_{exter}	V_{total}	V_{micro}
SAPO-37-W	14	/	/	0.03	/
Cu-SAPO-34-W	624	564	60	0.26	0.21

[a] Surface area and pore volume were determined by *t*-plot method.

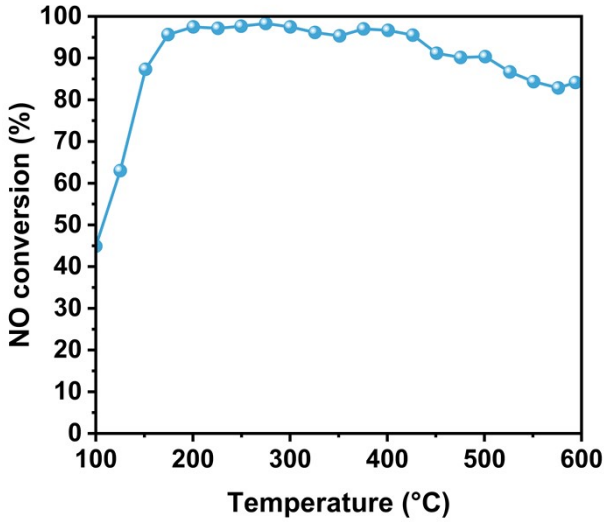

Fig. S22 NO conversion as a function of temperature for Cu-SAPO-34-W. Reaction condition: 5% O_2, 500 ppm NO, 500 ppm NH_3, balance N_2, GHSV=40000 h^{-1}.